arXiv:0907.1621v1 [cond-mat.mes-hall] 9 Jul 2009

Giant Surface Plasmon Induced Drag Effect (SPIDEr) in Metal Nanowires

Maxim Durach,[1] Anastasia Rusina,[1] and Mark I. Stockman[1,2,3]

[1] *Department of Physics and Astronomy, Georgia State University, Atlanta, Georgia 30303, USA*
[2] *Max Planck Institute for Quantum Optics, Hans-Kopfermann-Strasse 1, 85748 Garching, Germany*
[3] *Ludwig Maximilian University Munich, Am Coulombwall 1, 85748 Garching, Germany**

(Dated: July 9, 2009)

Here, for the first time we predict a giant surface plasmon-induced drag effect (SPIDEr), which exists under conditions of the extreme nanoplasmonic confinement. Under realistic conditions, in nanowires, this giant SPIDEr generates rectified THz potential differences up to 10 V and extremely strong electric fields up to $\sim 10^5 - 10^6$ V/cm. The SPIDEr is an ultrafast effect whose bandwidth for nanometric wires is ~ 20 THz. The giant SPIDEr opens up a new field of ultraintense THz nanooptics with wide potential applications in nanotechnology and nanoscience, including microelectronics, nanoplasmonics, and biomedicine.

The fact that electromagnetic fields exert mechanical forces on matter is well known and has found applications in atomic physics[1,2] and bio- and nanotechnology,[3,4,5] and picosecond photodetectors based on the photon drag effect (PDE).[6] The semiconductor PDE detectors have proved to be very practical for relatively fast detection of picosecond pulses in a wide frequency range spanning from THz to infrared. It has beeen proposed to use enhanced fields in phonon-polariton silicon carbide structures for laser particle accelerators.[7] There have been experimental investigations of the PDE in metal nanofilms that are thicker than the skin depth[8,9] Metals support surface plasmon polaritons (SPPs)[10] that exert forces on electrons causing an SPP-enhanced PDE.[8] However, it is typically rather small, with the induced potential differences in the mV range. This modest enhancement of the PDE in these experiments was due to relatively slow variation of SPP fields in space, and the momentum transferred to the electrons was correspondingly small. Because of the long relaxation times of the SPPs at plane metal surfaces, this PDE is also expected to be relatively slow. A drag effect under the conditions of strong nanoplasmonic confinement, when the SPP localization radius is less than the skin depth (~ 25 nm), has not been studied or exploited theoretically or experimentally.

In this Letter, we predict a giant surface plasmon-induced drag effect (SPIDEr) in metal nanowires, which is fast, with response on the femtosecond time scale. We show that the ultrashort, nanolocalized SPP pulses exert forces on electrons in the nanowires, inducing giant THz electromotive force (emf) along the SPP propagation direction. We have found that in thin (~ 5 nm radius) wires this emf can reach ~ 10 V, with nanolocalized THz fields as high as ~ 1 MV/cm. Such THz field have previouisly been generated in the far zone[11], where they produce non-perturbative effects,[12] but not on the nanoscale. In contrast, the plasmonic metal nanowires can serve as nanolocalized sources of high THz fields. We also study the dynamics of the SPIDEr for short SPP pulses and suggest that adiabatically tapered nanowires[13] can be used as broadband nanoscopic photodetectors with extremely fast response due to the femtosecond momentum

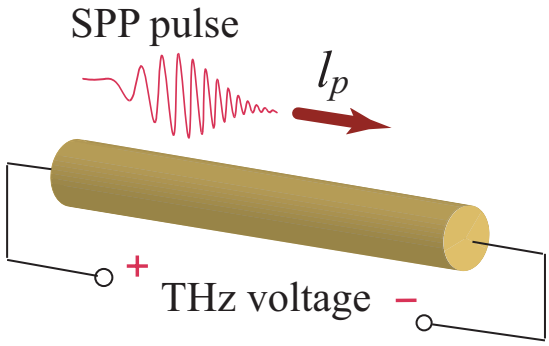

FIG. 1: Schematic of SPIDEr in metal nanowire. Propagating SPPs create forces acting on carriers in the nanowire, which leads to THz-band voltage (emf) between the ends of the wire. Picosecond or femtosecond pulses can be used to manipulate the time dependence of the created emf.

relaxation times in metals.[14] The nature of the giant enhancement of the SPIDEr is novel in nanoplasmonics: it is not the enhancement of the optical fields *per se* (the maximum magnitude of the local fields is limited by the breakdown at the metal surface that occurs for fields ~ 1 V/Å) but the very high *gradients* of these fields. The SPIDEr is ultrafast because it is a non-resonant effect whose bandwidth is comparable to that of the entire optical spectrum.

Consider a metal nanostructure propagating an SPP pulse. The SPP field produces polarization $\mathbf{P}$, charges with macroscopic density $\rho = -\mathrm{div}\mathbf{P}$, current density $\mathbf{j} = \partial\mathbf{P}/\partial t$, and the surface charge density $\sigma = (\mathbf{P}\cdot\mathbf{n})$ at the surface of the metal, where $\mathbf{n}$ is the normal to the surface pointing outward. We do not consider systems with optical magnetism, whose introduction at optical frequency is problematic[15,16] Therefore we set $\mathbf{B} = \mathbf{H}$, which precludes the existence of surface currents. Using Eqs. (6)-(8) of the Methods Section, we obtain the following general expression for the total force

$$\mathbf{F} = \int_V \left[\mathrm{grad}(\mathbf{P}^c \cdot \mathbf{E}) + \frac{1}{c}\frac{\partial(\mathbf{P}\times\mathbf{B})}{\partial t} \right] dV \ , \qquad (1)$$

where superscript "c" implies that the differentiation

does not apply to the labeled vector. This result is of fundamental importance for processes involving interaction of nanoplasmonic fields with metal electrons.[26] Equation (1) is valid for a wide range of problems with a general material equation $\mathbf{P} = \hat{\chi}\mathbf{E}$, including those where operator $\hat{\chi}$ describes anisotropic or non-local media. The first term in Eq. (1) is similar to the force acting on a point dipole moment.[17] The second term in Eq. (1) is the Abraham force. In a monochromatic field, this force averaged over the period of oscillations is zero, but in the field of a pulsed excitation it has a finite magnitude.

We apply this fundamental Eq. (1) to describe the SPIDEr. For certainty, consider a metal nanowire with radius R and dielectric susceptibility $\chi(\omega)$, which is oriented along the z-axis and embedded into a dielectric with a dielectric permittivity of ε_d. This wire propagates an SPP pulse, which can be excited by external sources using, e.g., the effect of adiabatic compression.[13,18]

In the case of extreme nanoplasmonic confinement ($R \ll l_s$, where l_s is the skin depth), R becomes the only relevant quantity of the dimensionality of length.[13] Therefore there is scaling of all magnitudes in R. The SPP wave power $\mathscr{P}$ scales as $\mathscr{P} \sim E^2R^2v_g$, where $v_g \sim \omega R$ is the SPP group velocity. The SPIDEr-induced potential difference [electromotive force (emf)] $\mathscr{E}$ is proportional to the pressure produced by force (1), $\mathscr{E} \sim F/R^2$. The propagation length of the SPP $l_p \sim RQ$, where Q is the SPP figure of merit, independent of R. These arguments allow us to predict scaling of the SPIDEr force F, emf $\mathscr{E}$, and the electric field due to SPIDEr rectification E_R (which for femtosecond SPP pulses possesses THz frequencies): $F \propto \mathscr{P}R^{-1}$, $\mathscr{E} \propto \mathscr{P}R^{-3}$, $E_R \propto \mathscr{P}R^{-4}$, $E_{mR} \propto R^{-1}$ .We have also indicated the scaling of the maximum rectified field E_{mR} (at the maximum tolerable power $\mathscr{P}_m$). The scaling implies that all the effects caused by the SPIDEr increase with decreasing the wire radius as its powers. This enhancement is not resonant and therefore has bandwidth comparable to that of the entire optical spectrum. The scaling describes only the dependence on R. There are also prefactors describing the dependence on dielectric permittivities, frequency, etc. They take into account an additional enhancement close to the SP resonant frequency, which is multiplicative in magnitude. Below in this paper we show that this scaling is reproduced by the theory results.

The SPPs are transverse magnetic (TM) modes, and their complex fields have the form

$$\mathbf{E} = A(t')(\tilde{E}_z\hat{\mathbf{z}}+\tilde{E}_\rho\hat{\boldsymbol{\rho}})e^{i(kz-\omega t)},\ \mathbf{H} = A(t')\tilde{H}_\varphi\hat{\boldsymbol{\varphi}}e^{i(kz-\omega t)}, \tag{2}$$

where $t' = t - z/v_g$, and v_g is the SPP group velocity at the pulse carrier frequency ω, k is the SPP wave number.[13] The total power flowing through the plane $z = 0$ at the moment t is $\mathscr{P}(t) = 2\pi\int_0^\infty \rho d\rho \bar{S}_z(\mathbf{r},t)|_{z=0}$, where $\bar{\mathbf{S}}(\mathbf{r},t) = (c/8\pi)\mathrm{Re}[\mathbf{E}\times\mathbf{H}^*]$ is the Pointing vector averaged over SPP period. Considering the azimuthally-symmetric (TM_0) modes, functions $\tilde{E}_z$, $\tilde{E}_\rho$ and $\tilde{H}_\varphi$ depend only on radius ρ. We normalize them for real amplitude $A(t)$ to satisfy a relation $A^2(t) = \mathscr{P}(t)$. Disregarding the group velocity dispersion in Eq. (2) is valid for pulses with duration of tens of femtoseconds and greater, and frequencies not too close to the SP resonance.

The momentum transferred from the electromagnetic field to the electronic system implies forces exerted on the electrons. The density of these forces are given by Eqs. (4) and (5) of the Methods Section. These forces lead to an emf, which corresponds to optical rectification in the system, which for femtosecond SPP pulses results in the emf in the THz frequency range. Since the electron momentum-relaxation time is on the scale of femtoseconds, electrons come to a local equilibrium in the process of this rectification. Therefore, we will describe it in the hydrodynamic approximation, for which the pressure p and electrostatic potential ϕ satisfy an equation $p + ne\phi = const$, where e is electron charge, and n is electron density. From this equation, we can find the emf $\mathscr{E} = \Delta\phi$, which is the total change of potential in the direction of SPP propagation (the z direction), $\mathscr{E} = -\Delta p/(ne)$, where $\Delta p = \bar{F}_z/(\pi R^2)$ is the full change of the pressure. Here, $\bar{F}_z$ is z-component of the force (1) averaged over the period of SPP oscillations.

The total force $\bar{F}_z$ is composed of three forces (see Eq. (9) in Methods Section): the SPP pressure, striction, and Abraham force $\bar{F}_z = f_z^{pr} + f_z^{st} + f_z^A$. These three forces result in three terms of the SPIDEr emf

$$\mathscr{E} = R_H\left(\frac{\mathscr{F}(t)}{A_{pr}} + \frac{\mathscr{P}(t)}{A_{st}} + \frac{\mathscr{F}'(t)}{cL_A}\right), \tag{3}$$

where $R_H = -1/(ecn)$ is the Hall constant, and coefficients A_{pr}, A_{st}, and L_A and $\mathscr{F}(t)$ are defined by Eqs. (10)-(13) of the Methods Section. The Abraham force contribution [the third term in Eq. (3)] is small under a condition $k_0l_p/(kc\tau) \ll 1$, where $k_0 = \omega/c$, and τ is the pulse duration. This condition is well satisfied for the parameters used in this paper. We will consider two limiting cases pertaining to Eq. (3): a quasi-monochromatic regime of long pulses ($\tau \gg t_p$) and a regime of short pulses ($\tau \ll t_p$), where t_p is the SPP dissipation time. Consider first the quasi-monochromatic regime where $\mathscr{F}(t) \approx \mathscr{P}(t)$ (see Eq. (10) of the Methods Section). In such a case, the total emf $\mathscr{E}(t)$ follows the pulse-envelope time dependence $\mathscr{P}(t)$. The computations will be made for a silver[19] nanowire embedded in vacuum ($\varepsilon_d = 1$).

For the quasi-monochromatic case, the total emf $\mathscr{E}$ as a function of frequency ω and wire radius R is displayed in Fig. 2 (a). In contrast to the case of dielectric media, in the present plasmonic case the SPP pressure and striction contributions to the emf have the same sign since $\chi' < 0$. These two contributions are equal if a condition $\chi''Q = -\chi'$ is satisfied. The black solid line represents this condition; to the left of this line the pressure dominates, and to the right the striction force gives the major contribution to the SPIDEr. This is understandable because close to the SP resonance of the wire (at ≈ 3.7 eV), the gradient of the SPP intensity increases due to the high loss: the striction force is of a gradient nature,

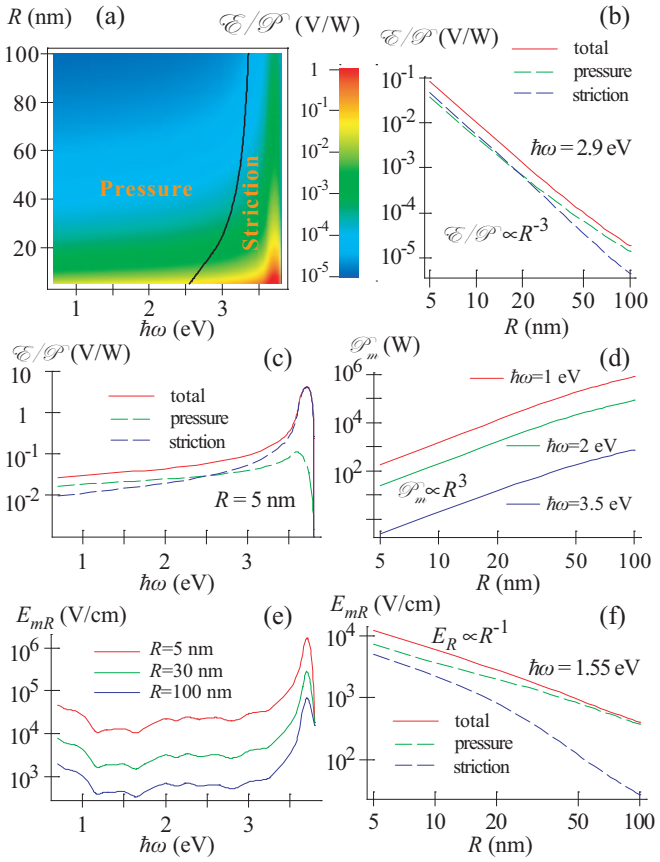

FIG. 2: SPIDEr for quasi-monochromatic SPP pulses: emf and rectified field dependence on the frequency $\hbar\omega$ and wire radius R. Note the logarithmic scale for the magtnitude of the effect. (a) Dependence of the SPIDEr emf per unit SPP power $\mathscr{E}/\mathscr{P}$ on wire radius and frequency. The black broken curve indicates the parameters at which SPP pressure is equal to striction. The magnitude of the effect is denoted by the color-coding bar. (b) Dependence of SPIDEr magnitude $\mathscr{E}$ on wire radius R per unit power of the SPP wave (solid red curve). The contributions of the pressure and striction to the total magnitude of SPIDEr are shown by the dashed curves. (c) Dependence of SPIDEr magnitude per unit power $\mathscr{E}/\mathscr{P}$ on frequency ω for $R = 5$ nm. (d) Maximum power that a wire can tolerate $\mathscr{P}_m$ as a function of wire radius R for different frequencies ω. (e) The maximum SPIDEr rectified field E_{mR} (for the maximum tolerable power $\mathscr{P}_m$) as a function of frequency for three wire radii $R = 5$, 30, and 100 nm. (f) The maximum SPIDEr rectified field E_{mR} (for the maximum tolerable power $\mathscr{P}_m$) as a function of the wire radius R for frequency $\hbar\omega = 1.55$ eV.

dominating therefore. Similarly, with the decrease of R, the intensity gradient increases due to the increased confinement, which also leads to the relative increase of the striction with respect to the pressure force, as we clearly can see from this and other panels of Fig. 2. General increase of the SPIDEr at the SP resonant frequency can be seen as a broad red peak.

Magnitude of the SPIDEr emf relative to the SPP wave power, $\mathscr{E}/\mathscr{P}$, is illustrated in Fig. 2 (b) as a function of the wire radius R for a frequency of $\hbar\omega = 2.9$ eV. The SPIDER effect is gigantically enhanced for strong nanoplasmonic confinement: by four orders of magnitude when R decreases from 100 to 5 nm at the same SPP power. There is a pronounced scaling $\mathscr{E}/\mathscr{P} \propto R^{-3}$ at $R \lesssim l_s$, in accord with the discussion following Eq. (1).

The spectral dependence of the relative SPIDER emf, $\mathscr{E}/\mathscr{P}$, for a wire of the smallest radius considered, $R = 5$ nm, is depicted in Fig. 2(c).[27] Importantly, the magnitude of the emf in this case is very large, from 0.01 to 10 V per 1 W of the SPP pulse power, in the entire optical range, with a pronounced resonance at the SP frequency. This large magnitude shows that the SPIDEr effect can be used for the photodetection on the nanoscale, i.e., in the role that previously was deemed only available for semiconductors. In this sense, it belongs to the area of the active nanoplasmonics.[20]

By classification of the nonlinear optics, the SPIDEr is an optical second-order nonlinear effect: the magnitude of the SPIDEr emf $\mathscr{E}$ is proportional to the power $\mathscr{P}$ of the SPP field. Therefore, the maximum achievable magnitude of the emf is determined by the maximum $\mathscr{P}$ that the wire can tolerate. This we estimate setting the optical field E at the surface of the wire equal to 1 V/Å.[21,22] For fields significantly higher than this, there will be massive ionization and damage of the metal surface. We plot in Fig. 2 (d) this maximum intensity as a function of the wire radius for three SPP frequencies. Note a very good scaling $\mathscr{P}_m \propto R^3$ in the region $R \lesssim l_s$ of the strong nanoplasmonic confinement. These values of the $\mathscr{P}_m$ in comparison to the data of Fig. 2 (a)-(c) show that the gigantic values of of the SPIDEr emf $\mathscr{E} \sim 10$ V are realistically achievable, which are many orders of magnitude greater than observed previously in the metal films.[8,9]

One of the most important for applications properties of the giant SPIDEr is high local electric field E_R generated due to the SPIDEr optical rectification in the vicinity of the nanowire. Such a field (averaged over the SPP decay length l_p) can be found as $E_R = \mathscr{E}/l_p$. We display the maximum achievable rectified field E_{mR} (at the propagating SPP power of $\mathscr{P}_m$) in Figs. 2 (e), (f). As we see from panel (e), the spectral dependence of the SPIDEr rectified THz field is very similar for all wire sizes, but the magnitude of this field is much greater for the 5 nm wire: $E_{mR} \sim 10^5 - 10^6$ V/cm. The nanolocalized THz fields of such a magnitude will excite a wealth of nonlinear THz responses at the nanoscale.

Now let us consider dynamics of the emf response to SPP pulses that differ in duration τ with respect to the the SPP pulse dissipation time t_p. The latter is displayed in Fig. 3 (a) as a function of the frequency ω. As we can see time t_p is in the range from 10 to 150 fs. The temporal dependencies of the emf in comparison with the power $\mathscr{P}$ of the SPP pulses for various pulse durations is illustrated in Figs. 3 (b)-(d). For a relatively long pulse ($\tau = 1$ ps $\gg t_p$) shown in Fig. 3 (b), the shape of the emf $\mathscr{E}(t)$ repeats that of the power $\mathscr{P}(t)$. This relatively long, picosecond response, nevertheless, corresponds to a

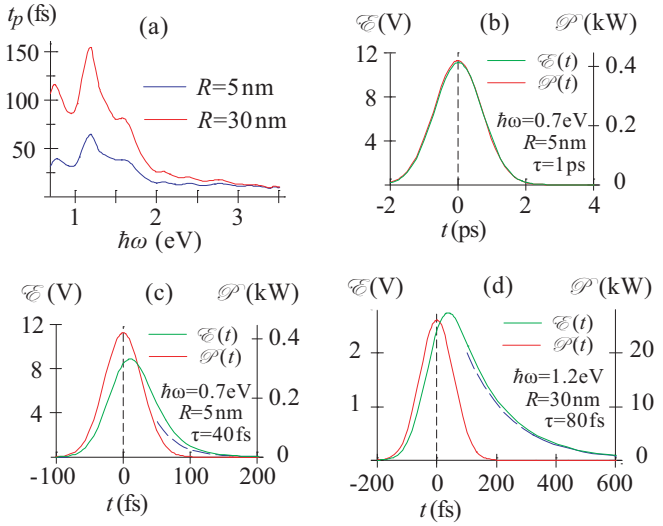

FIG. 3: SPIDEr created by ultrashort SPP pulses: fast femtosecond emf response. (a) The dependence of the SPP lifetime $t_p = l_p/v_g$ on the frequency $\hbar\omega$ for $R = 5$ nm and $R = 30$ nm. (b) The time dependence of the emf $\mathscr{E}(t)$ (green line, left scale) and input power $\mathscr{P}(t)$ (red line, right scale). The pulse duration is $\tau = 1$ ps $\gg t_p \approx 30$ fs and the emf closely follows the SPP pulse dynamics. (c) The same for much shorter pulse with $\tau = 40$ fs. The pressure-induced emf leads to small broadening in emf dynamics (green line). The limiting exponential decay is outlined by the broken blue line. (d) Emf induced by the short pulse in nanowire with $R = 30$ nm with frequency $\hbar\omega = 1.2$ eV. The emf response is broadened, since $\tau = 80$ fs, while $t_p \approx 150$ fs.

1 THz bandwidth for this nanowire used as a nanoscale photodetector. Note that the amplitude of the emf is very large, ~ 10 V.

For a much shorter, $\tau = 40$ fs, SPP pulse and the same 5 nm wire, as shown in Fig. 3 (c), there is a small broadening and delay of the voltaic response (emf) $\mathscr{E}(t)$ with respect to the excitation SPP pulse $\mathscr{P}(t)$. This broadening is due to the pressure force that decays exponentially for long times, as Eq. (10) of the Methods Section suggests, and the broken blue line in the figure indicates. However, under the conditions considered, this delay and broadening are not large. The frequency-response bandwidth of this wire as an SPP photodetector on the nanoscale is very large, ≈ 20 THz, which is characteristic of the extreme nanoplasmonic confinement. The amplitude of the SPIDEr emf is also very large, $\mathscr{E} \sim 10$ V.

For a much thicker nanowire of $R = 30$ nm (weak plasmonic confinement case) and $\hbar\omega = 1.2$ eV, illustrated in Fig. 3 (d), the SPP decay time becomes much longer ($t_p = 150$ fs). This leads to a very significant delay and temporal broadening of the emf response with a pronounced exponential part due to the pressure forces shown by the broken blue line. These behavior is due to the much longer SPP lifetimes for the weak confinement where a significant fraction of the SPP energy propagates in the dielectric (vacuum). Nevertheless the emf response bandwidth is still very large, on the order of 5 THz, and its amplitude is also very large, $\mathscr{E} \gtrsim 1$ V.

In conclusion, the ultrafast giant SPIDEr in metal nanowires excited by ultrashort SPP pulses is predicted in this Letter to generate a gigantic emf up to ~ 10 V for the SPP waves of realistic and tolerable amplitudes. The SPIDEr enhancement is mostly nonresonant, due to nanoplasmonic confinement of the SPP fields, which leads to higher gradients of the fields and their higher magnitudes. Because of its nonresonant nature, the SPIDEr is an extremely fast effect: frequency bandwidth of the generated THz fields is realistically 5-20 THz. Due to high longitudinal localization of the SPP waves in the case of the strong nanoplasmonic confinement, the SPIDEr generates very high local THz electric fields at the metal surface, $E_R \sim 10^5 - 10^6$ V/cm. Such fields are capable of inducing strongly nonlinear responses, including dissociation of molecules. Among possible applications of the giant SPIDEr are rectification and detection of the nanoscale femtosecond optical fields, coupling of the nanoplasmonic elements to semiconductor devices, nonlinear THz spectroscopy on the nanoscale of chemical and biological nanoobjects for biomedicine, etc.

This work was supported by grants from the Chemical Sciences, Biosciences and Geosciences Division of the Office of Basic Energy Sciences, Office of Science, U.S. Department of Energy, a grant CHE-0507147 from NSF, and a grant from the US-Israel BSF. MIS work at Garching was supported under contract from Ludwig Maximilian University of Munich (Germany) in the framework of Munich Center of Advanced Photonics (MAP). MIS gratefully acknowledges stimulating discussions with F. Capasso regarding photoinduced potentials in near-field optical microscope tips.

Methods

Then a macroscopic (averaged) Lorentz force density inside the material volume is given by

$$\mathbf{f}^v = -\mathbf{E}(\nabla \cdot \mathbf{P}) + \frac{1}{c}\frac{\partial \mathbf{P}}{\partial t} \times \mathbf{B} \ . \tag{4}$$

The surface polarization charges experience the Lorentz force with a surface density

$$\mathbf{f}^s = \sigma \mathbf{E} \ . \tag{5}$$

The volume force density given by Eq. (4) can be represented in the following way

$$\mathbf{f}^v = -\mathrm{div}\,(\mathbf{P} \otimes \mathbf{E}) + \mathrm{grad}(\mathbf{P}^c \cdot \mathbf{E}) + \frac{1}{c}\frac{\partial(\mathbf{P} \times \mathbf{B})}{\partial t} \ , \tag{6}$$

where $\otimes$ denotes the outer product of vectors. Thus, the total force acting on the polarization charges in the SPP field is

$$\mathbf{F} = \int_V \mathbf{f}^v \, dV + \oint_S \mathbf{f}^s \, ds \ , \tag{7}$$

where the first integration runs over volume V of the structure, and the second is over its surface S. Noticing that the volume integral of the first term in Eq.(6) is equal to

$$-\int_V \mathrm{div}\,(\mathbf{P}\otimes\mathbf{E})\,dV = -\oint_S (\mathbf{P}\cdot\mathbf{n})\mathbf{E}\;ds = -\oint_S \mathbf{f}^s\;ds\;, \tag{8}$$

we cancel terms in Eq. (7) to simplify it and obtain the required Eq. (1) of the paper.

From Eq. (1) of the paper, the total force acting on electrons can be expressed as a sum of the SPP pressure, striction, and Abraham force, whose z-components are, correspondingly,

$$f_z^{pr} = \frac{\pi R^2 \mathscr{F}(t)}{cA_{pr}}\;,\quad f_z^{st} = \frac{\pi R^2 \mathscr{P}(t)}{cA_{st}}\;,\quad f_z^{A} = \frac{\pi R^2 \mathscr{F}'(t)}{c^2 L_A}\;, \tag{9}$$

where

$$\mathscr{F}(t) = \frac{1}{l_p}\int_0^\infty \mathscr{P}(t')e^{-z/l_p}dz = \\ = \frac{e^{-t/t_p}}{t_p}\int_{-\infty}^{t} \mathscr{P}(t')e^{t'/t_p}dt'\;. \tag{10}$$

In Eq. (9), coefficients A_{pr} and A_{st} have dimensionality of area, and L_A has dimensionality of length. They are defined as

$$A_{pr} = \left(\frac{c\chi'' Q}{2R^2}\int_0^R |\tilde{\mathbf{E}}|^2\rho d\rho\right)^{-1}\;, \tag{11}$$

$$A_{st} = -\left(\frac{c\chi'}{2R^2}\int_0^R |\tilde{\mathbf{E}}|^2\rho d\rho\right)^{-1}\;, \tag{12}$$

$$L_A = \left(\frac{cl_p}{R^2}\int_0^R \mathrm{Re}\left(\chi\tilde{E}_\rho\tilde{H}^*_\varphi\right)\rho d\rho\right)^{-1}\;, \tag{13}$$

where $Q = \mathrm{Re}k/\mathrm{Im}k$ is the SPP figure of merit, $|\tilde{\mathbf{E}}|^2 = |\tilde{E}_\rho|^2 + |\tilde{E}_z|^2$, $l_p = 1/(2\mathrm{Im}\,k)$ is the SPP propagation length, and $t_p = l_p/v_g$ is the SPP pulse lifetime.

* Electronic address: mstockman@gsu.edu; URL: http://www.phy-astr.gsu.edu/stockman

1 T. W. Hänsch and A. L. Schawlow, Optics Communications **13**, 68 (1975).
2 V. S. Letokhov, V. G. Minogin, and B. D. Pavlik, Soviet Physics - JETP **45**, 698 (1977).
3 A. Ashkin and J. M. Dziedzic, Science **235**, 1517 (1987).
4 L. Novotny, R. X. Bian, and X. S. Xie, Physical Review Letters **79**, 645 (1997).
5 V. Giovanni, Q. Romain, B. Goncal, and P. Dmitri, Phys. Rev. Lett. **96**, 238101 (2006).
6 S. Ganichev and W. Prettl, *Intense Terahertz Excitation of Semiconductors* (Oxford University Press, 2006).
7 S. Kalmykov, O. Polomarov, D. Korobkin, J. Otwinowski, J. Power, and G. Shvets, Phil. Trans. Royal Soc. A **364**, 725 (2006).
8 A. S. Vengurlekar and T. Ishihara, Applied Physics Letters **87**, 091118 (2005).
9 T. Hatano, B. Nishikawa, M. Iwanaga, and T. Ishihara, Opt. Express **16**, 8236 (2008).
10 *Plasmonic nanoguides and circuits* (2008).
11 A. Sell, A. Leitenstorfer, and R. Huber, Opt. Lett. **33**, 2767 (2008).
12 S. Leinss, T. Kampfrath, K. von Volkmann, M. Wolf, J. T. Steiner, M. Kira, S. W. Koch, A. Leitenstorfer, and R. Huber, Phys. Rev. Lett. **101**, 246401 (2008).
13 M. I. Stockman, Phys. Rev. Lett. **93**, 137404 (2004).
14 V. V. Kruglyak, R. J. Hicken, M. Ali, B. J. Hickey, A. T. G. Pym, and B. K. Tanner, Physical Review B **71**, 233104 (2005).
15 L. D. Landau and E. M. Lifshitz, *Electrodynamics of Continuous Media* (Pergamon, Oxford and New York, 1984).
16 R. Merlin, Proc. Natl. Acad. Sci. USA **106**, 1693 (2009).
17 Y. Shimizu and H. Sasada, American Journal of Physics **66**, 960 (1998).
18 E. Verhagen, A. Polman, and L. Kuipers, Opt. Expr. **16**, 45 (2008).
19 P. B. Johnson and R. W. Christy, Phys. Rev. B **6**, 4370 (1972).
20 K. F. MacDonald, Z. L. Samson, M. I. Stockman, and N. I. Zheludev, Nat. Phot. **3**, 55 (2009).
21 B. Gault, F. Vurpillot, A. Bostel, A. Menand, and B. Deconihout, Applied Physics Letters **86**, 094101 (2005).
22 G. Sha, A. Cerezo, and G. D. W. Smith, Applied Physics Letters **92**, 043503 (2008).
23 M. I. Stockman, L. N. Pandey, L. S. Muratov, and T. F. George, Phys. Rev. Lett. **72**, 2486 (1994).
24 I. A. Larkin and M. I. Stockman, Nano Lett. **5**, 339 (2005).
25 J. Aizpurua and A. Rivacoba, Phys. Rev. B **78**, 035404 (2008).
26 We calculate *macroscopic* forces assuming that the nanostructure is homogeneous enough and the frequencies under consideration are far enough from the surface plasmon (SP) resonances. Then the field fluctuations, characteristic of the disordered systems,[23] could be disregarded.
27 For significantly thinner wires, nonlocal-response effects may become significant, cf. Refs. 24,25